Brazing and laser welding of a Ni-Cr alloy

PAULO CÉZAR RIOLI DUARTE DE SOUZA , JOSÉ CÍCERO DINATO**, MARCO ANTÔNIO BOTTINO***, ANTÔNIO CARLOS GUASTALDI*****

ABSTRACT

The purpose of this study was to analyse the microstructure and the hardness of a Ni-Cr alloy used in prosthetic dental restorations welded by brazing and laser. In the brazing process different microstructures were obtained for the base metal and for the weld zone, and in the laser welding three microstructure regions were found: the weld fusion zone, the heat affected zone – HAZ, and the base metal. The base metal showed a coarse dendritic microstructure and a eutectic interdendritic structure; the brazing weld presented a coarse dendritic morphology with extensive areas of precipitates and porosity, and a fine dendritic microstructure was found in the laser weld. The microstructures obtained were in accordance with the welding heat inputs. The laser welding traction tests results were superior to those obtained by the brazing weld. The weld zone hardness was bigger than the base metal's in both welding processes, the HAZ hardness was smaller than the base metal's, and its length was less than 1 mm due to the low energy transferred to the base metal. The use of laser welding in prosthetic pieces of reduced thickness shall not cause any significant distortion, being very promising to replace brazing in this application.

UNITERMS

Laser welding, brazing; gold alloy; silver alloy; prosthesis.

SOUZA, P. C. R. D. et al. Soldagem de uma liga de Ni-Cr empregando-se brasagem e laser. **Pós-Grad Rev Fac Odontol São José dos Campos**, v.3, n.2, p., jul./dez. 2000.

RESUMO

Investigou-se a microestrutura e a dureza de uma liga de NiCr utilizada em próteses odontológicas soldadas com brasagem e a laser. Verificou-se que na brasagem o metal base e o cordão de solda apresentaram microestruturas distintas, e que na soldagem a laser identificou-se três regiões: o cordão de solda, a zona afetada pelo calor - ZAC e o metal base. O metal base da liga NiCr apresentou uma microestrutura dendrítica grosseira com uma estrutura eutética interdendrítica, a região da solda por brasagem apresentou uma morfologia dendrítica grosseira com a presença de precipitados e porosidades e na soldagem a laser uma estrutura dendrítica refinada. Estas microestruturas foram condizentes com as energias de soldagem fornecidas em cada processo. Os resultados dos ensaios de tração da solda a laser foram superiores aos obtidos para a solda por brasagem. Para ambos os processos de soldagem a dureza no cordão de solda foi maior do que o metal base, na soldagem a laser a dureza na ZAC foi menor do que no metal base, e sua extensão foi menor que 1mm devido à pequena energia transferida ao metal base. O emprego da soldagem a laser em peças protéticas de pequenas espessuras não deverá causar distorção significativa, sendo promissor na substituição da brasagem nesta aplicação.

UNITERMOS

Soldagem a laser; brasagem; liga de Ni-Cr; prótese fixa; biomateriais.

* Dr. Eng., Pesquisador Instituto de Química de Araraquara/UNESP - CP. 355 – 14.800-900 – Araraquara – SP.
** Aluno de Pós-Graduação (Nível Doutorado) – Área Implantologia - Faculdade de Odontologia de Florianópolis – UFSC.
*** Departamento de Materiais Odontológicos e Prótese Faculdade de Odontologia de São José dos Campos - UNESP – 12245-000 – São José dos Campos - SP
**** Instituto de Química de Araraquara/UNESP - CP. 355 – 14.800-900 - Araraquara – SP.

Introduction

Nickel-Chromium alloys can be used to make fixed prosthesis, covered with resin or ceramics, clinic applications that require thin covers, due to its capacity to resist a great variety of operational conditions involving corrosive environment, high temperatures, mechanic efforts or any combination of these factors.

Besides the economic advantages, the Ni-Cr alloys advantages compared to the noble metals alloys include higher flow-off tension and traction resistance, high elasticity module, high resistance to flow and lower density. On the other hand, the disadvantages are high hardness, high melting temperature and greater difficulty to melt and weld[14].

The Ni-Cr alloys are different as to their composition, with nickel percentages varying from 70 to 80%, and chromium between 13 e 22%[12]. The main elements that can be present in these alloys composition are carbon, iron, magnesium, beryllium, molybdenum, aluminum, silicon, tungsten, boron and titanium.

The welding technique has the advantage of allowing work on segments of the prosthesis, reducing possible failures[9] during the making of the metal structure and even after the application of ceramics, and it has been a resource used in solving real problems.

Dentistry has employed for this purpose the brazing process with gas/air blowtorch, known as conventional welding, due to the low cost and technical facility, being the most used in the prosthetic laboratories. In this process the welding is carried out through an addition metal, with melting point lower than the base metal's, which does not melt during the welding, the joint being fulfilled by capillary effect [5,15]. The welded joint can be defined as the area where the union of two metallic parts takes place, with or without any addition metal, using a source of heat.

By the end of the 80's, the laser welding process was introduced in Dentistry with the development of smaller equipment, which bring operational facility and accessible cost. In Brazil, laser welding was introduced in 1997 [8], and has been used to replace the other welding processes in making dental prosthesis. Such process can be employed to weld a wide variety of metals, as well as different materials [5,15], due to the coherent, monochromatic, focused and high-energy light beam, without causing substantial distortions to the prosthetic piece.

The nickel alloys require attention during the welding, since they are susceptible to small differences in composition, to pre-heating, to high heat input, to the joint configuration and to its cleanliness[3].

The metallurgic problems associated to the welding of nickel and its alloys include porosity in the weld, precipitation of fragile phases and loss of resistance to corrosion, due to the formation of intragranular precipitates[1,3,11].

The porosity during welding can be avoided by using deoxidizing and nitrides forming elements or by using a protection atmosphere of inert gas. The main elements added for this purpose are aluminum and titanium, since they present great affinity with nitrogen and oxygen.

In brazing Ni-Cr alloys one can apply flows, which also promote the protection of the welded joint. According to Sobieralski et al.[14], regardless of the brazing process used, the flows are efficient in cleaning the welded area, reducing porosity.

The present study's goal is to investigate the response of the microstructure and the mechanical properties of a Ni-Cr alloy used in making dental prosthesis, before and after being submitted to the brazing and laser weld processes.

Materials and Methods

The Ni-Cr alloy used in this study is specifically for dental application. Its chemical composition and the one of the addition metal used in brazing are described in Table 1.

Preparation for metallography and hardness

The specimens, in the shape of an 11mm long, 4mm wide and 1,5mm thick plate, were submitted to the welding process in joints of the top type.

In order for the brazing to take place in the proper manner, the specimens were fixed so as to obtain a

Table 1 – Chemical Composition of the Ni-Cr alloy and of the addition metal (% m/m)

Elements	Ni-Cr alloy	Brazing addition metal
Ni	76,67±0,82	85,70±0,96
Cr	13,75±0,28	7,76±0,74
Al	2,25±0,03	0,07±0,01
Mo	4,45±0,20	_
Be	1,90±0,31	_
Fe	_	3,27±0,11
Ti	0,42±0,06	_
Si	0,05±0,01	3,12±0,28

breach in the joint of approximately 0,25mm. First they were joined with resin and then positioned in moulds of refractory material. Following, they were taken to the oven at 400^{0}C for 30min for the resin to burn. The space previously occupied by the resin was fulfilled with the recommended consumable, Table 1, and the specimens were brazed using a LPG blowtorch.

The laser welding was carried out on a Dentaurum DL 20002S machine, specific for dental application, which uses a Nd:YAG crystal as a laser source, applying a beam power of 5,04 kW for 12 milliseconds, as per manufacturer's recommendation, generating a welding energy of 60,48 J.

With the help of a device the specimens were positioned inside the chamber with argon protecting atmosphere, and from 35 to 40 welding spots were made on each side of the longitudinal section of the joint. In this section the welding spots were superposed on approximately 2/3 of their surfaces, so as to obtain a complete weld also in depth. The welding power applied was enough for the beam to penetrate around 60% in each side in the transversal direction of the joint.

After the welding, the specimens were cut, covered with resin, sandpapered, polished with granulation alumina of 1µm and 0,3µm and attacked with aqua regia, proportion in volume 2HCl:1HNO_3. The metallographic observation of the welded joints' transversal section was made through SEM-sweeping electronic microscopy with spectroscopy analysis through dispersing energy of X-rays - DEX.

The hardness tests on the base metal and welded joint were made with a hardness micrometer Micromet 2003, Buehler - USA. The samples were prepared in a way similar to the one used in the metallographic tests. The prints were made on a line parallel to the surface of the samples' transversal section, so as to analyze the response of the hardness in the base metal, in the heat-affected zone and in the weld.

Preparation for the Traction Tests

The specimens were obtained from wax moulds using a machine-made matrix, following the specification of International Standards Organization - ISO 6871. The process by lost wax was carried out in the equipment for melting by induction Ducatron-Series 3 using argon as protection gas and optic pyrometer to control melting temperature at 1350±20^{0}C.

A total of 18 specimens have been melted and divided in three groups: a) melted without weld, reference; b) laser welded e c) weld by brazing. The specimens of groups b e c were cut in the middle by a cutting disc to be welded using the procedures previously described.

Results and Discussion

The input energy is an essential element to the welding process, but, on the other hand, it may

represent a source of problems due to its direct influence on the metallurgic transformations and mechanical properties such as contraction and expansion, which occur in the weld zone. The lower the welding energy and temperature gradient between the melted pond and the adjacent region, the higher the cooling speed imposed will be[4,15].

The process of brazing with a blowtorch transfers great welding energy to the piece to be welded, generating a bigger heat-affected zone – HAZ - in the metal and causing bigger distortion problems in the pieces. The laser welding is a process whose peculiarity is a concentrated source of heat; therefore it minimizes such problems.

For the conditions used in the laser welding, the welding energy and the cooling speed have been estimated using the equations proposed by the American Welding Society [4,15] for thin plates, Table 2.

For the LPG, the average power in the blowtorch edge is 717J/cm^2 and the temperature is approximately 2750^{0}C [11]. Considering a 1mm^2 area, which is the approximate area covered by the laser beam, and a total brazing time of 60s, there is also an estimate welding energy and cooling speed for brazing, as shown in Table 2.

Table 2 shows that the laser welding releases a welding energy lower than the brazing welding, and consequently presents faster cooling speed.

Figure 1 shows the Ni-Cr alloy base metal /weld interface produced by brazing, where one notes that the brazing addition metal has shown good wetting capacity, since it has completely fulfilled the joint. One can observe, in the base metal, a gross melting dendritic microstructure with a eutectic phase in the interdendritic region, and, in the weld zone, a dendritic microstructure (clear phase) with porosity and precipitates. Figure 2 shows the same region more amplified, identifying two kinds of precipitates, one clearer (CP) another a little darker (DP) on which were made the DEX punctual analysis.

Figure 2 shows the base metal and weld zone interface area, where the elementary mapping was made. Figures 3 to 6 show the mapping of the elements Ni, Cr, O e Mo respectively, the white spots corresponding to the presence of the mapped elements and the black spots may correspond to the absence of the element or to the porosities observed in Figure 2.

Table 2 – Welding energy and cooling speed estimates in the Ni-Cr alloy laser welding and brazing processes

Welding process	Welding energy (J)	Cooling speed (^{0}C/s)
Laser	60,48	2,91. 10^3
Brazing	430,2	57,47

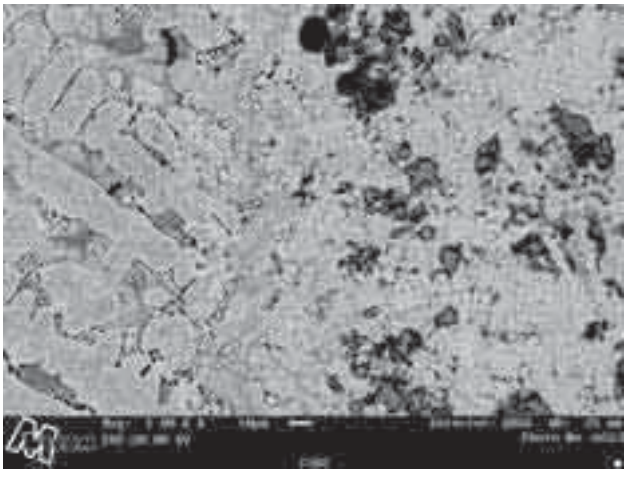

FIGURA 1 - Brasagem: microestrutura da interface metal base (MB) / cordão de solda (CS); Ataque: água régia; 1000X.

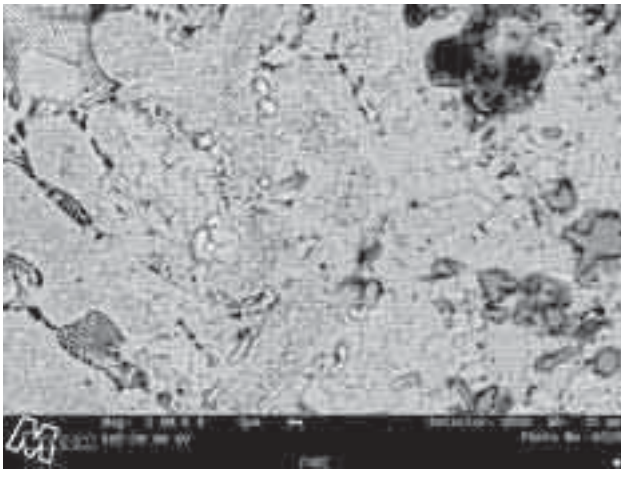

FIGURA 2 - Brasagem: Microestrutura da interface metal base (MB) / cordão de solda (CS), na qual foi realizada a técnica de mapeamento elementar; Ataque: água régia; 2000X

The nickel mapping, in Figure 3, shows that it is uniformly distributed along the base metal and the brazing weld, and no difference in concentration of this element has been detected either in the dendrites' arms or in the surrounding region, due to the DEX technique limitation. One can also note that the nickel is virtually absent from the precipitated particles, which are shown as the black spots in Figure 3.

The Cr mapping, Figure 4, shows that this element is present in all micrography, but it has higher proportions in both precipitates found in the weld zone, especially in the dark particles. The O mapping, Figure 5, indicates that this element is also present in higher proportion in the dark particles along with the Cr.

In the Mo mapping, Figure 6, one can see that this element is present in both precipitates, but shows higher concentration in the clear particles.

Therefore, one can infer, from the information obtained in the elementary mapping, that the dark particles can be a chromium-molybdenum oxide, and the clear particles an intermetallic of Cr-Mo. The presence of these oxides and the porosity is a consequence of the contamination by gases, especially oxygen, during the brazing process with a blowtorch.

Figure 7 shows the microstructure of the base metal /weld zone interface produced in the Ni-Cr alloy laser welding. In this Picture the base metal shows a gross microstructure of coarse dendritic melting with interdendritic spaces united by a eutectic lamellar structure. In the base metal the dendrites show arms between 10 and 30 mm thick.

In the weld zone a fine dendritic microstructure has been obtained, noting in Figure 7 that these have been cored with the base metal and oriented in the direction of the thermal flow during the cooling process, from the base metal to the weld zone core. Figure 8 shows the microstructure of the weld zone, in which we can verify that the dendrites' arms are approximately 1mm thick and the space between dendrites is smaller than 0,5mm.

The microstructure obtained in the Ni-Cr alloy brazing was correspondent to the higher welding energy released and the lower cooling speed originated by the latter, Table 2, since it has produced a microstructure coarser than the laser welding.

The fine dendritic microstructure found in the laser welding was due to the overcooling imposed by the process, since as the solidifying rises it establishes a condition of instability in the solid/liquid interface growth, originating the flat structures followed by the cellular and dendritic structures, in a similar way to the structures found in an ingot cooling[4,10,15].

Table 3 shows the results of the traction tests for the three conditions studied: "as received", laser welded and welded by brazing. One notes that the "as received" condition has shown greater deformity and tension values until rupture, followed by the laser welded and welded by brazing conditions.

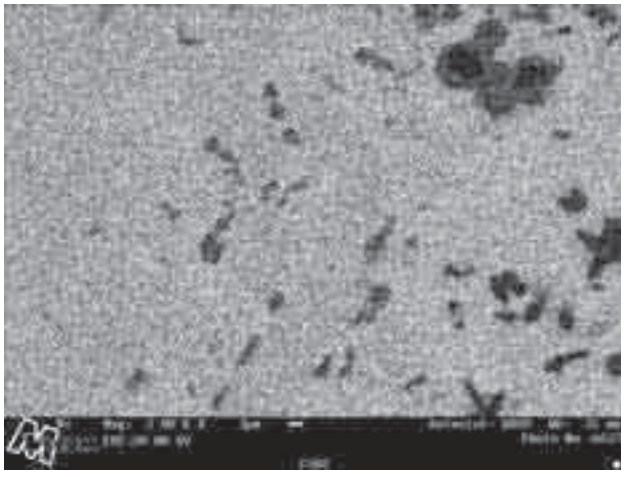

FIGURA 3 - Brasagem: mapeamento do elemento níquel da liga Ni-Cr; 2000X.

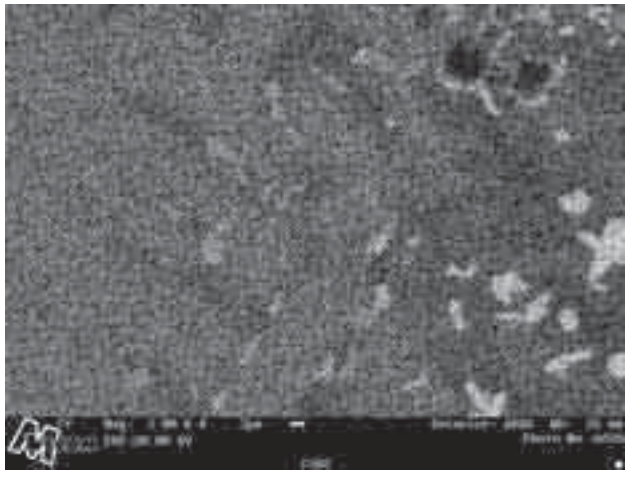

FIGURA 4 - Brasagem: mapeamento do elemento cromo da liga Ni-Cr;2000X.

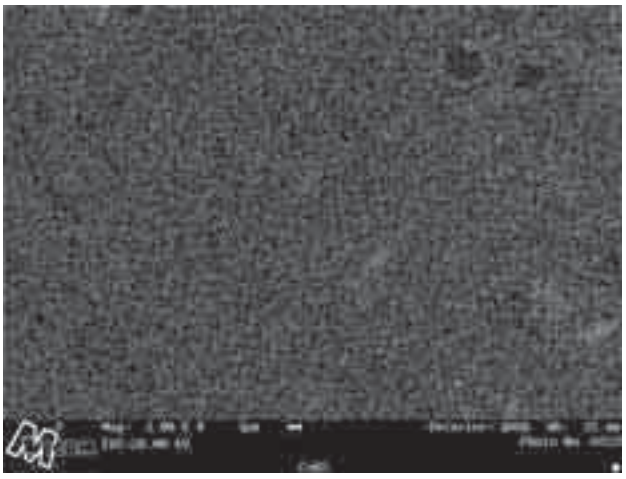

FIGURA 5 - Brasagem: mapeamento do elemento oxigênio da liga Ni-Cr; 2000X.

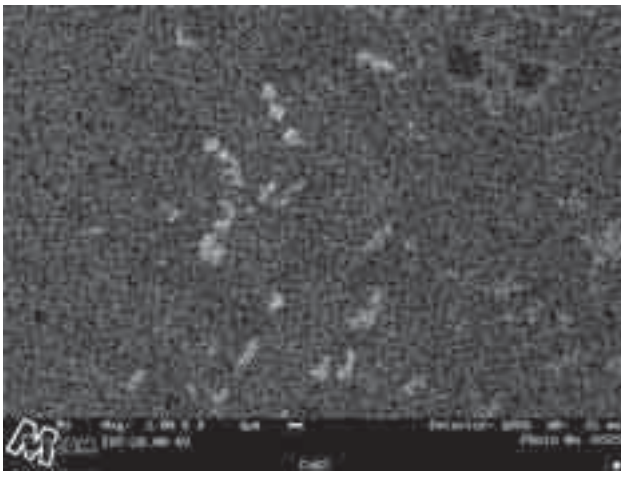

FIGURA 6 - Brasagem: mapeamento do elemento molibdênio da liga Ni-Cr; 2000X.

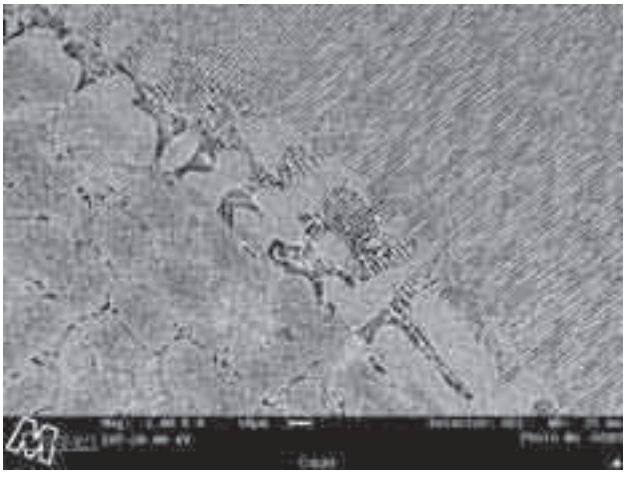

FIGURA 7 - Laser Microestrutura da interface metal base (MB)/ cordão de solda (CS); Ataque: água régia; 1000X.

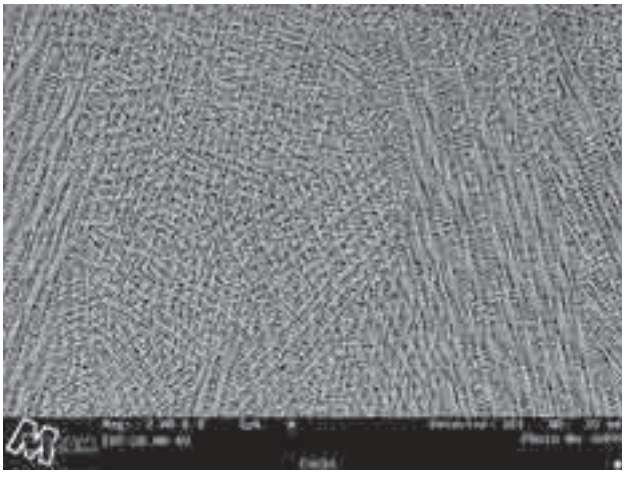

FIGURA 8 - Laser: Microestrutura do centro do cordão de solda; Ataque: água régia; 2000X

Table 3 - Results on the Ni-Cr alloy traction tests

Condition	Rupture Tension (MPa)	Deformation (%)
Melted	1006 ± 29	0,18
Laser welded	749 ± 145	0,08
Welded by brazing	299 ± 126	0,03

Figures 9 to 17 show the fracture micrography of the traction tests. Figure 9 shows the transversal section of the test piece after the test for the melted without weld condition, and Figures 10 and 11 show in further details that region, which presents a mixed fragile/ductile fracture, with predominance of interdendritic fracture [2].

Figure 12 shows the transversal section of the test piece after the test for the welded by brazing condition, where we can see porosity and two kinds of fractures, interdendritic and fragile. Figure 13 shows the region where there is a mixed fragile/ductile fracture with predominance of interdendritic fracture, and Figure14 shows the region

where we have a predominantly fragile fracture, with cleavage areas [2,13].

Figure 15 shows the transversal section of the specimen after the test for the laser welded condition, where we can see the lack of penetration of the laser beam, originating a welding failure in its core. Analyzing the fracture in this region, Figures 16 and 17, one verifies that it shows the characteristic of a mixed fragile-ductile fracture by tearing, where the microcavities break and coalesce with the fissure vertex [2,13].

Figures 18(a) e 18(b) show the hardness profiles of the transversal section of the specimens welded by brazing and laser respectively, and Table 3 shows the average hardness values obtained. In Figure 18(a) and Table 3 one notices that in the brazing weld the hardness was bigger in the weld zone than in the base metal. The average hardness in the welded region was very high, 580 HV, way above the recommended values for this alloy application, from 290-350 HV [12]. The high hardness in the welded region can be explained by the presence of the precipitates and oxides, which have caused hardening by precipitation in this region, since the Ni alloys are susceptible to this hardening mechanism, especially when they show concentrations higher than 1% of aluminum or titanium[4,6]. The elevated hardness combined with the presence of porosity tend to turn the welded region more fragile, making the brazing process not recommendable for this kind of application.

Analyzing Figure 18(b) and Table 3, we verify that in the laser welding the hardness, although higher in the weld zone than in the base metal and in the HAZ, can be considered statistically identical for these three regions. One can also see that the HAZ formed in the laser welding process is small, less than 1mm.

Although the laser welding has presented welding failures due to the technique employed, the traction tests results were superior to the ones obtained by brazing. Based on these results, combined with the small HAZ formed due to the lower energy provided by the laser beam to the base metal, one can affirm that this process should not cause significant distortion to the welding of prosthetic pieces of reduced thickness, being very promising to replace brazing.

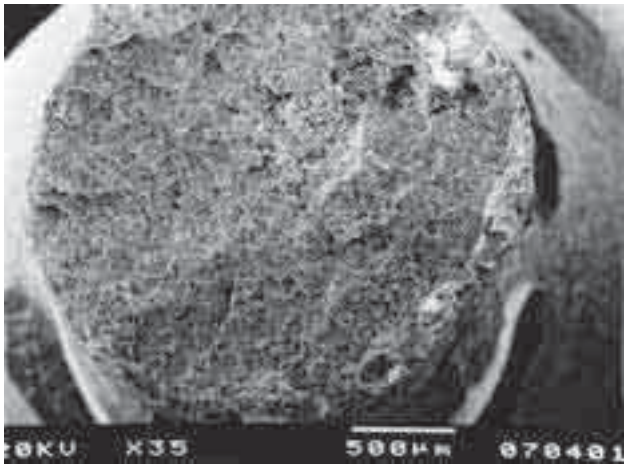

FIGURA 9 - MEV da fratura do corpo-de-prova na condição fundido sem solda; Aumento 35X.

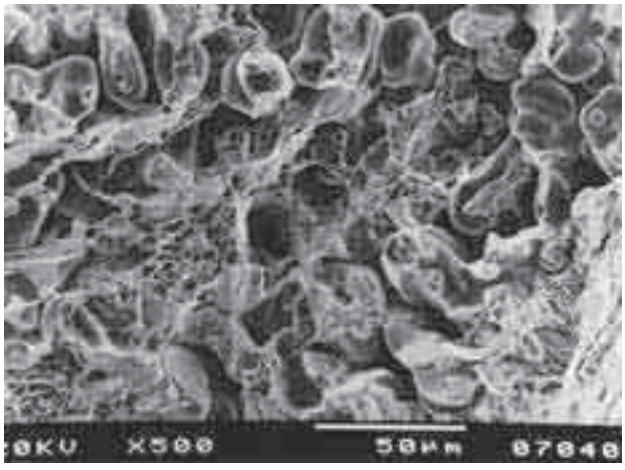

FIGURA 10 - MEV da fratura interdendrítica no corpo-de-prova na condição fundido sem solda; 500X.

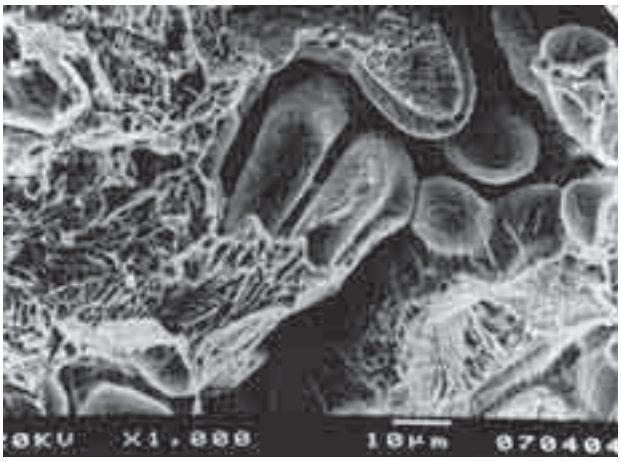

FIGURA 11 - MEV da fratura interdendrítica no corpo-de-prova na condição fundido sem solda; 1000X.

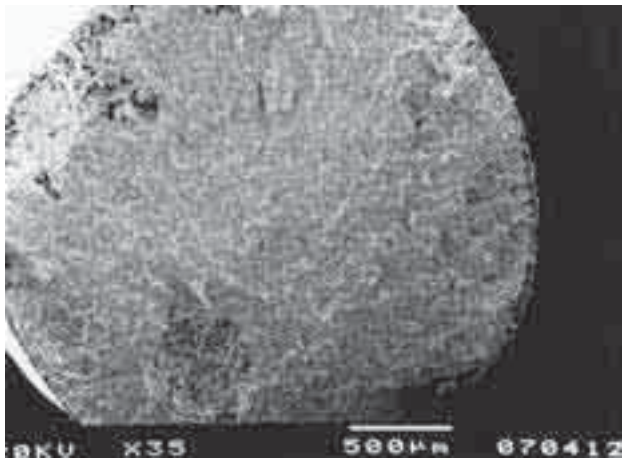

FIGURA 12 - MEV da fratura do corpo-de-prova na condição soldado por brasagem; 35X.

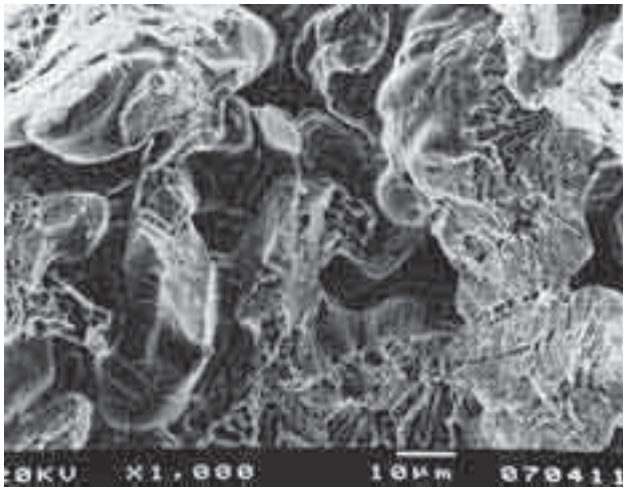

FIGURA 13 - MEV da fratura interdendrítica no corpo-de-prova na condição soldado por brasagem; 1000X.

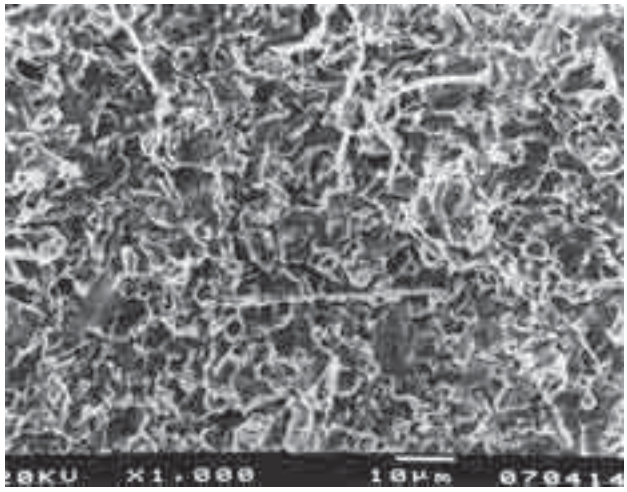

FIGURA 14 - MEV da fratura frágil no corpo-de-prova na condição soldado por brasagem; 1000X.

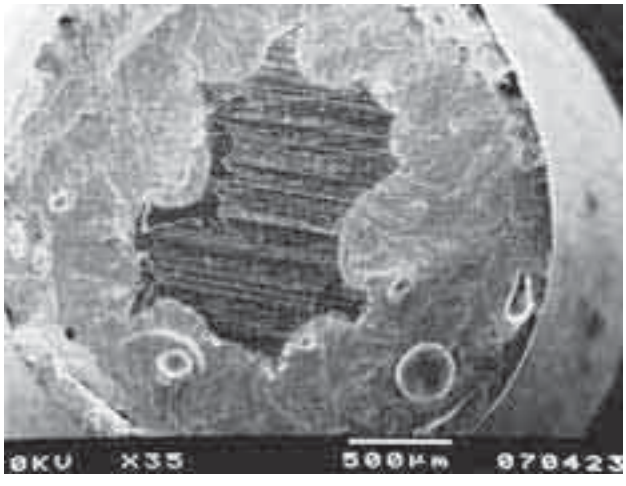

FIGURA 15 - MEV da fratura do corpo-de-prova na condição soldado a laser, mostrando a solda com porosidades e a região central com falha de soldagem; 35X

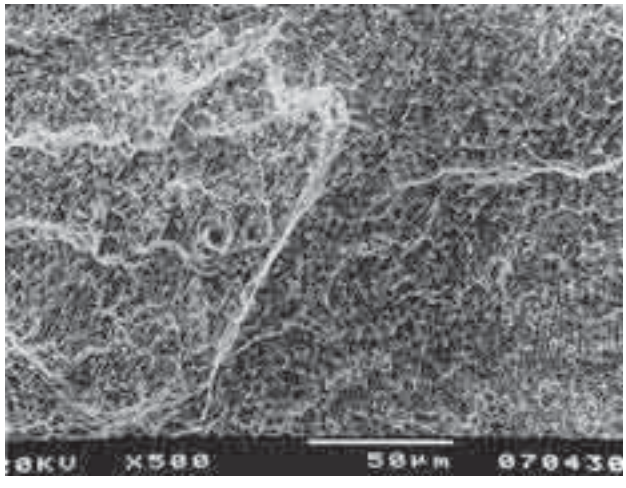

FIGURA 16 - MEV da fratura dúctil por rasgamento do corpo-de-prova na condição soldado a laser; 500 X.

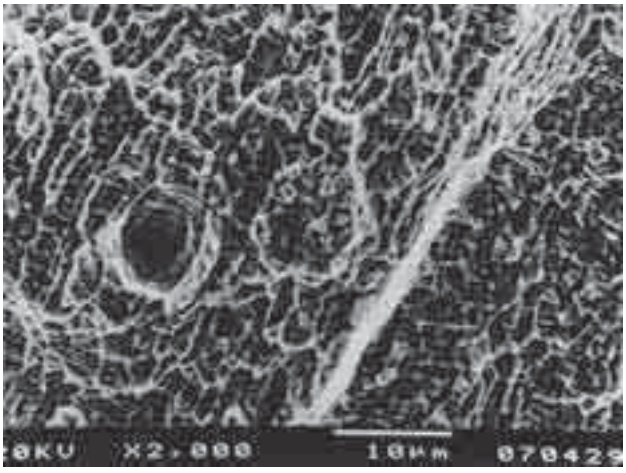

FIGURA 17 - MEV da fratura dúctil por rasgamento do corpo-de-prova na condição soldado a laser; 2000X.

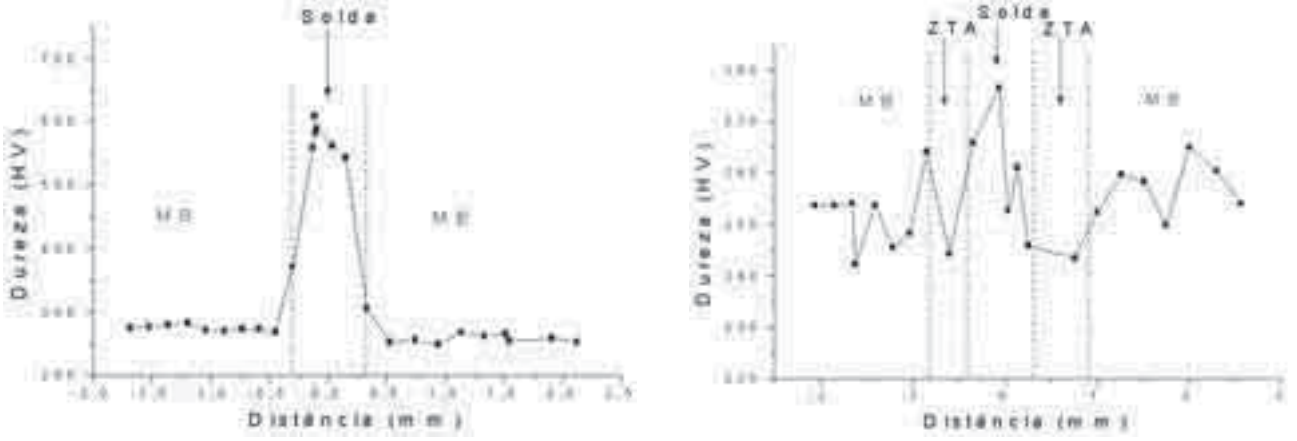

FIGURA 18 - Perfil de dureza da secção transversal com relação ao centro da solda; (a) brasagem (b) solda a laser; MB= metal base , ZAC = zona afetada pelo calor.

Table 4 – Hardness measures of the Ni-Cr alloy welded joint

Region	Hardness (HV)	
	Brazing	Laser
Base Metal	266 ± 10	253 ± 7
Welded Zone	579 ± 41	258 ± 12
HAZ	-	246 ± 25
HAZ Extent (mm)	-	0,6

Conclusions

The conclusions are:

a) the base metal microstructure presents a coarse dendritic morphology with the presence of a microstructure of the eutectic kind in the interdendritic region;

b) in the laser welding we have obtained a fine dendritic microstructure in the weld zone;

c) in the brazing welding a coarse dendritic microstructure has been obtained, with the presence of porosity and precipitates, identified as being of Cr-Mo and Cr and Mo oxides through the DEX analysis;

d) the microstructures obtained in the laser and brazing welding have been coherent with the cooling speed imposed by those processes;

e) one notes that the "as received" condition has shown higher deformation and tension values until rupture, followed by the laser welded and welded by brazing conditions;

f) the hardness in the weld zone region was greater than in the base metal for the two welding processes, being the high hardness in the brazing welding above the values recommended for this application;

g) the concentrated high-energy laser beam has provided a low heat input to the base metal, minimizing the size of the HAZ, less than 1mm, and as a consequence there shall be no distortion to the prosthetic pieces;

h) to minimize the failures in the laser welding the operator shall establish an adequate joint project and determine precisely the penetration of the laser beam.

Acknowledgment

We would like to thank **FAPESP** for the financial support of the Post-Doctorate scholarship **(Proc.98/11096-7)** and the Projeto de Auxílio à Pesquisa **(Proc. 98/16415-3)**.

Bibliographic References

1. AMERICAN SOCIETY FOR METALS. **ASM metals handbook –**Metals Park: American Society for Metals, 1992. p.1014-21, (Walding Brazing and soldering, v.6).

2. AMERICAN SOCIETY FOR METALS. **ASM metals handbook –** Metals Park: American Society for Metals, 1992, (Fractography, v.12).

3. AMERICAN WELDING SOCIETY. **Introductory welding metallurgy**. 3 ed., Miami: American Welding Society, 1979. cap. 4.

4. AMERICAN WELDING SOCIETY. **Welding handbook-**, Miami: American Welding Society, 1982. v.1, cap. 1-4.

5. AMERICAN WELDING SOCIETY. **Welding handbook-** Miami: American Welding Society, 1987. v.2, cap. 12, 22.

6. BRICK, R.M. et al. **Structure and properties of alloys**. 3∞ Ed. New York: McGraw-Hill, 1965.

7. BUMGARDNER, J.D.; Lucas, L.C. Cellular response to metallic ions released from nickel-chromium dental alloys. **J. Dent. Res.**, v.74, n.8, Aug. p.1521-7, 1995.

8. DINATO, J. C. et al. **Flexural resistance of dental alloys submitted to laser and conventional welding compared**. In: Annual Meeting of the Academy of Osseointegration, 13, Atlanta, 1998, Proceedings: Georgia, USA, march 5-7.

9. DINATO, J. C. et al. **Chemical, microstructural and hardness analisys of laser welded for implant prostheses alloys**. In. Annual Meeting of the Academy of Osseiointegration, 14, New Orleans, 1999, March.

10. IERARDI, M.C. et al. Aspectos induzidos por fusão superficial com laser em aço ferramenta. **Metalurgia & Materiais**, v.51, n.6, p.522-7, jun., 1995.

11. MARQUES, P. V. **Tecnologia da soldagem**. Belo Horizonte: ESAB, 1991. cap. 1, 9, 14.

12. PHILLIPS, R. W. **Skinner materiais dentários**, 9 ed. Rio Janeiro: ed. 1993. Guanabara Koogan, caps. 4, 13, 20, 27.

13. SEABRA, A. V. Fractografia: seu interesse técnico e económico. **Ciência & Tecnologia dos Materais,** v.10, n.1-2, p.11-23,1998.

14. SOBIERALSKI, J.A.; BRUKL, C.E.; SMITH, N.K Tensile strengths and microscopic analysis of nickel-chromium base metal postceramic solder joints. **J. Prosthet. Dent.**, v.58, n.1, p.35-42, July 1987.

15. WAINER, E. et al. **Soldagem:** processos e metalurgia. São Paulo: Ed. Edgar Blucher, 1992.